The 2018 World Congress on
Advances in Civil, Environmental, & Materials Research (ACEM18)
Songdo Convensia, Incheon, Korea, August 27 - 31, 2018

Exploration of tube segment uplift through a full-scale model test of immersed tube tunnel foundation treated by sand-flow method

Yadong LI[1)], *Wei LI[2)] and Jie CUI[3)]

[1)]*School of Civil Engineering, Guangzhou University,*
230 Wai Huan Xi Road,GuangZhou Higher Education Mega Center, Guangzhou, China
[2)] *South China University of Technology, School of Civil Engineering and Transportation,*
Wushan RD., Tianhe District, Guangzhou, China
[*]*lyd9999@qq.com*

ABSTRACT

A full-scale model test of an immersed tube segment with a dimension of 8.2 m ×15.2 m has been carried out for the exploration of tube segment uplift in the process of sand-flow foundation treatment. The amount of tube uplift, the radius of sand deposit, the water pressure and trench gap and the structural form of sand deposit were obtained through the real-time monitoring of sand deposit and the observation of sand deposit digging. The tube uplift mechanism, sand deposit extension rules, gap water pressure and sand deposit morphological were discussed in detail. Results showed that the increase of trench gap water pressure and the change of sand particle deposition modes were the direct causes of tube uplift. The process of tube uplift could be divided into three sub-stages (pulsatile-up, rapid-up and smooth-up stages). It was also found that the tube uplift process had no effect on the pressure of sand pump outlet; the uniformity of sand deposit extension would influence the expanding rate of sand deposit radius significantly; the peak value of water pressure and the commence of tube uplift were determined by the weight of tube; the compactness of sand deposit was between loose and medium dense; the uplift of the model board could compact the sand deposit.

1. INTRODUCTION

Immersed tunnel, one kind underwater tunnel to across rivers and straits in city, with special application scopes and intrinsic limitations, is mainly applied to river and sea with soft soils (Kuesel 1986). Immersed tunnel have been widely used in the world (Grantz 2001a, Grantz 2001b, Nestor 1997), due to series of advantages such as abundant section shapes, better construction safety, excellent waterproof property, and

---

[1)] Assistant Professor
[2)] Engineer
[3)] Professor

low requirement for conditions of engineering geology and construction (Sun 2006). Foundation treatment is an important node in immersed tunnel construction, which directly correlated many quality problems of emplacement inaccuracy, foundation settlement and liquefaction. The sand-flow method has already been one of the most popular processing methods for immersed tunnel foundation treatment because of its advantages (Glerum 1995).

The sand-flow method was firstly used in the foundation treatment for Vlake tunnel in Netherlands (Van 1978). In the process of construction, the inlet pressure, sand deposit radius and sand volume were monitored and tested, which provided real constructional experience for sand-flow method. A scale of 1:5 model test for the process parameters including the radius of sand deposit, the void ratio of sand deposit, and the pressure of sand-flow was carried out prior to the construction of Guangzhou Biological Island-University City Tunnel. A full scale model test for Zhoutouzui immersed tunnel foundation treatment using sand-flow method was conducted in 2013 (Li 2013, Fang 2012, Mo 2012). In the test, the general process and the sand deposit structural characteristics were explored, and some unique structures on the deposit, such as sand deposit, crater, flow gaps, flow chutes, and oblique bedded texture were described. It was also demonstrated the influence of construction parameters and boundary conditions on sand deposit extension.

Previous studies had explored the principles of sand-flow method, examined the parameters of design and construction, and provided the references for the immersed tunnel construction. However, till now there is no related research works published on the tube segment uplift in foundation treatment resulting from sand-flow method and the influence on the construction of immersed tunnel. In the design scheme, it is clearly put forward a standard operation that the starting point of tube segment uplift as the ending point of construction, obviously, the rationality is questionable. Therefore, it is necessary to carry out the test to study the rules and quantitative parameters on tube segment uplift in foundation treatment by sand-flow method.

Based on the project of Zhoutouzui immersed tunnel foundation treatment, a full scale model test for sand-flow method in water beneath was carried out in this study. The whole process of tube segment uplift in sand-flow foundation treatment was simulated. A series of suitable reaction parameters such as the amount of tube uplifting, the radius of sand deposit, the water pressure of system and trench gap and the structural form of sand deposit were obtained through the real-time monitoring of sand deposit and the observation of sand deposit digging. The tube uplift mechanism, sand deposit extension rules, gap water pressure and sand deposit morphological were discussed in detail. The amount and rate of uplifting were obtained from experiment. The process of tube segment uplift could be divided into three sub-stages according to the mechanical characteristics of model board, the patterns and structural characteristics of sand deposit. The reason for formation of crater, flow gaps, flow chutes and oblique bedded texture and theirs features were introduced. Moreover, the causes of tube segment uplift were analyzed according to the deposition mode of sand deposit and the phenomenon of water pressure increase. Finally, several suggestions to tube uplift control, treatment for flow gaps and chutes, propagation of sand deposit were rendered. The results gained through this study can be applied as references for the design and construction of similar engineering projects.

2. ENGINEERING BACKGROUND

The Guangzhou Zhoutouzui immersed tunnel with 340-meter-long which including main tubes of E1 (85 m), E2 (85 m), E3 (79.5 m) and E4 (90.5 m). Among them, E1 and E4 tube sections are variable cross-section tube segments. The project layout of Zhoutouzui immersed tunnel is shown in Fig. 1. The sketch map of E1 tube segment size and sand deposit design is shown in Fig. 2.

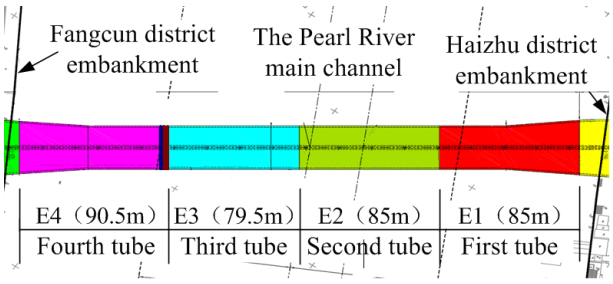

Fig. 1 Project layout of Zhoutouzui immersed tunnel

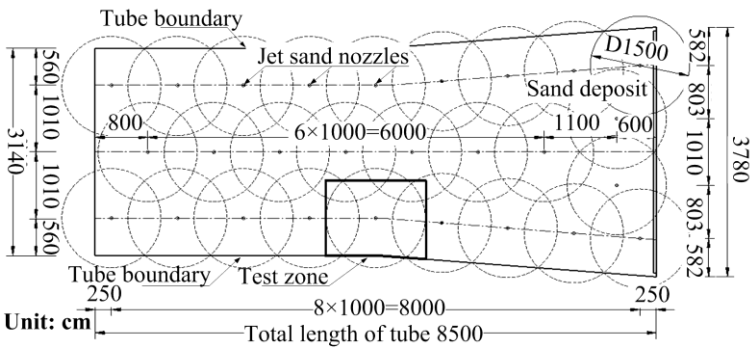

Fig. 2 Sketch map of E1 tube segment size and sand deposit design

According to the design documents on Zhoutouzui immersed tunnel, the sand-flow foundation treatment should meet the following requirements:
(1) After each tube is located, the trench gap should be filled with gravel coarse sand by the sand-flow method to form an artificial sand deposit foundation. The design distance between centers of sand deposits should be 10.0 m.
(2) The vertically jacking forces and tube segment position should be real-time monitored during the construction process. When the force is reaching to the warning value or the tube position changes, the construction should be suspended immediately and then emergency measures should be taken to ensure tube anti-floating stability.
(3) Construction parameters including time and pressure of sand perfusion, expanding radius should be determined by model test before construction. According to the reliable test results, the design radius of sand deposit should be adjusted to a rational level.

3 Experiment on sand-flow method

3.1 Test System

Based on Guangzhou Zhoutouzui immersed tunnel project, within one sand deposit, a test system consisting of model, equipment and measurements were established to evaluate the foundation treatment by sand-flow method (Li 2013, Li 2014). Test simulation zone as the thick solid region is shown in Fig.2.

3.1.1 Model

The experimental model system was composed of model board, circulating tank, underground reservoir, etc. (as shown in Fig.3). The size of the reinforced concrete model board was 820 cm×1520 cm, and it was located in the test tank to simulate the floor within a single hole in the condition of underwater. The 1.0 m trench gap was for the simulation of the groove gap at tunnel bottom.

(a)

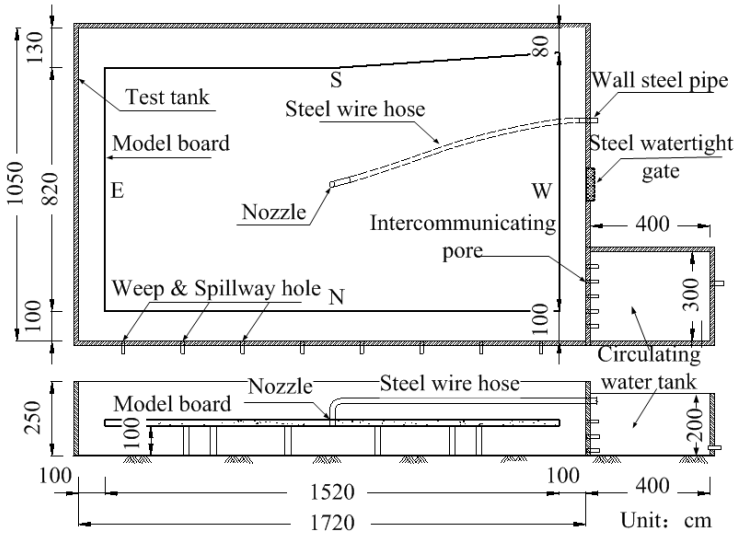

(b)

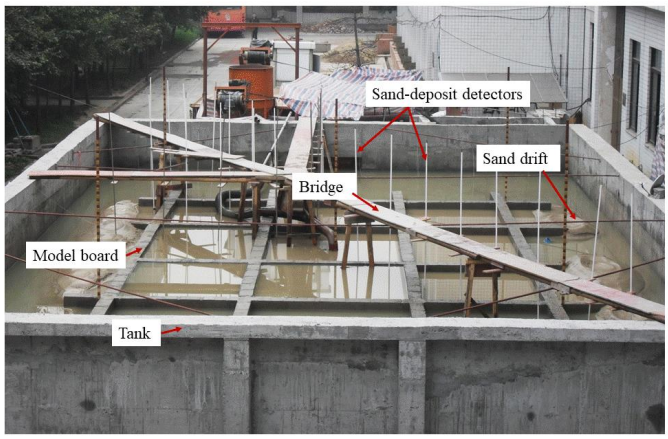

Fig. 3 Sketch map of E1 tube segment size and sand deposit design. (a) Sketch map, (b) Photo of model test

3.1.2 Equipment

The test equipment system as a guarantee of stable sand-flow for the test was composed of four major parts as quantitative water conveyance, quantitative sand conveyance, sand water injection and control system, which included equipment as water pumps, butterfly valve, return valve, sand conveyer belt, sand reservoir, sand distributor, sand-water blender, sand pump and control cabinet. The layout of test equipment system is shown in Fig. 4.

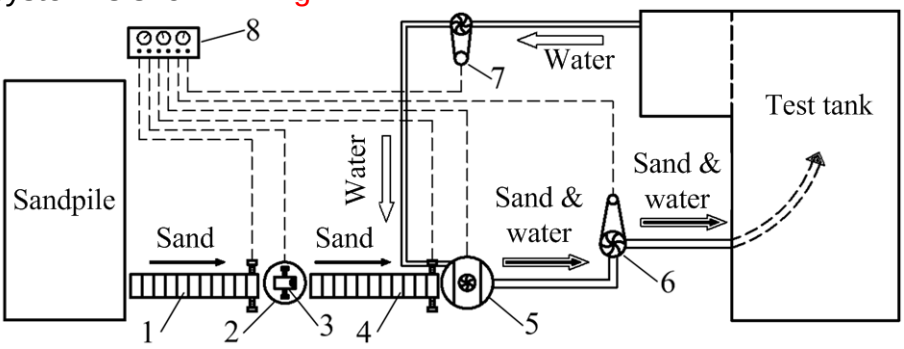

Note: 1-First conveyor belt; 2-Sand container; 3-Sand material distributor; 4-Second conveyor belt; 5-Sand-water blender; 6-Sand pump; 7-Water pump; 8-Control cabinet.

Fig. 4 Layout diagram of equipment system

3.1.3 Measurement

The real-time data of sand deposit extension was measured by the sand detectors installed on the X, Y axis of model board. The layout and parameters of measurement system are shown in Fig. 5 and Table. 1. The time-history curves on the height and radius of sand deposit can be figured out from the data of each measuring point at different time.

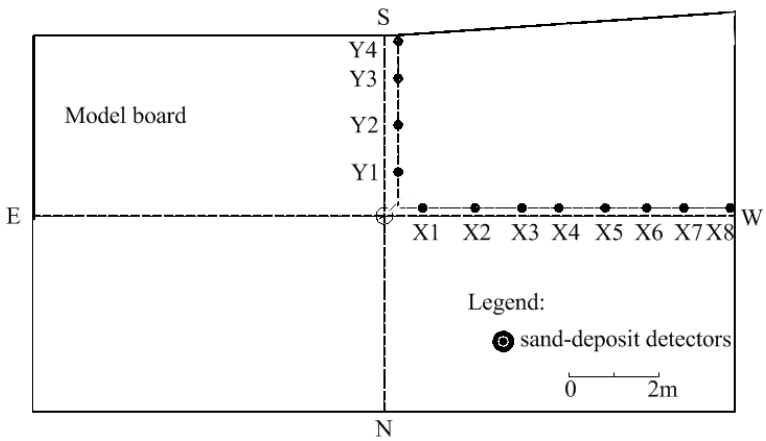

Fig. 5 Layout diagram of sand-deposit detectors

Table. 1 Position of sand-deposit detectors

Axis	Measuring Posts							
	1	2	3	4	5	6	7	8
X (m)	0.9	2.0	3.0	3.8	4.8	5.7	6.5	7.5

Y (m)	1.0	2.0	3.0	3.8	/	/	/	/

The real-time water pressure in trench gap was measured by the water pressure gauge mounted on the model board bottom. The layout of gauges is shown in Fig. 6. The model board uplifting process was real-time measured by the displacement posts P_{WN}, P_{EN}, P_{ES}, P_{WS} and P_C. The final uplifting value of model board was measured through the supporting corner columns (Z_{WN}, Z_{EN}, Z_{ES} and Z_{WS}) and sand nozzle pressure. The layout of measuring points is shown in Fig. 6.

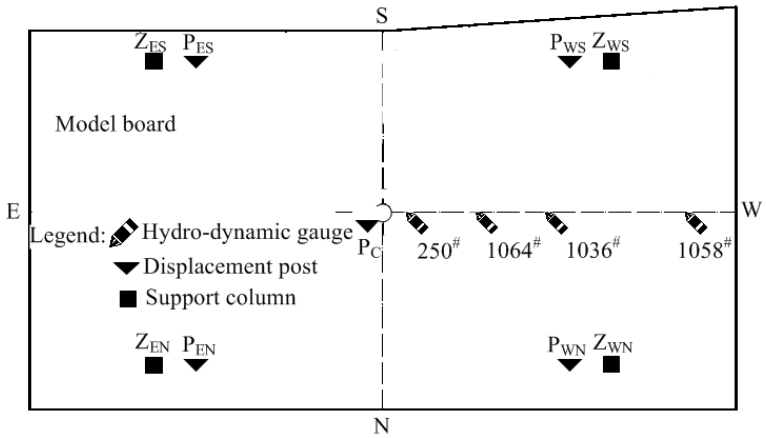

Note: Hydro-dynamic gauges were installed on the model board undersurface, the displacement post was installed on the model board surface, and the support column was located under the model board.

Fig. 6 Layout diagram of hydro-dynamic gauge, displacement post and support column

3.2 Test sand

The density of sand for experimental test is 2.641g/cm^3, the medium grain diameter D_{50} and natural repose angle of sand were 0.61 mm, 33.4°. The sand grading curve was obtained by screening test, and the result is shown in Fig. 7.

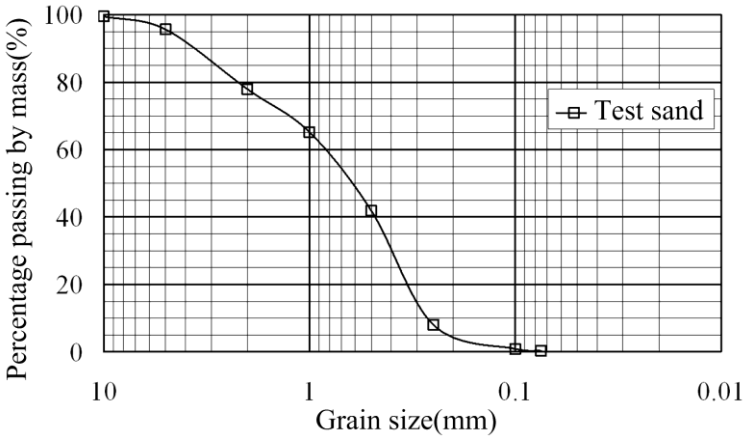

Fig. 7 Grain size accumulation curve of the test sand

3.3 Test parameters

According to the project experience of Guangzhou Biological Island-University City Tunnel, Hollandsch Diep Service Tunnel, District Heating Tunnel and Oude Maas Service Tunnel (Nestor 1997), the ratio of sand to water was selected as 1:10 to 1:7, the height of the trench gap was set as 0.6 m to 1.0 m (Nestor 1997). In the tube segment uplifting test (T-UP test), the mass ratio of sand to water was controlled to 1:9, a value close to the engineering practice, through the adjusting control of pump valve, return valve and sand material dispenser. The 1.0 m gap between the board and ground was for the simulation of the trench gap of immersed tunnel floor. The T-ST control test was as a reference, which model board was fixed on the basement by pull rod, uplifting was forbidden during test, and the gap between board and the ground was 0.8 m.

4. TEST RESULTS

The amount of model board uplifting, radius and height of sand deposit and water pressure of gap between board and ground were measured in the test. The uplifting amount of corner columns, the consistency and structure characteristics of sand deposit were obtained through the digging of sand deposit.

4.1 Model board uplifting process

The tank level could be used as the datum plane of measurement for its constant even the water level up to the overflow hole. The uplifting amount of model board uplifting can be measured by the post P_{WN}, P_{EN}, P_{ES}, P_{WS}, P_C.

Fig. 8 shows the time-history curves of tube segment uplifting and tank water level.

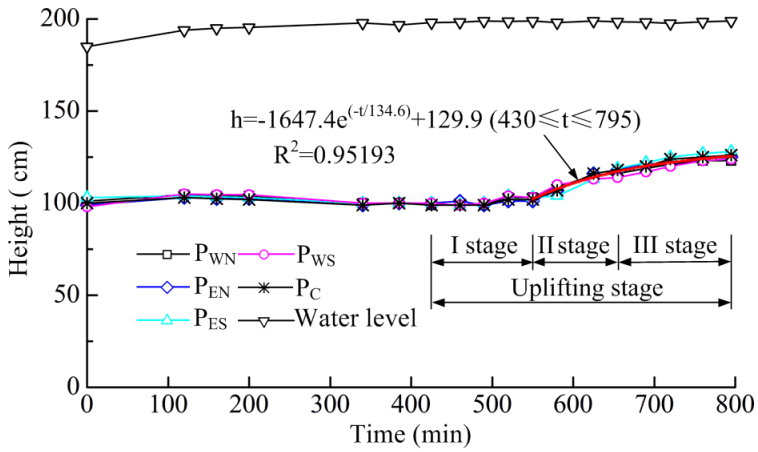

Note: The maximum uplifting amounts of each measuring point are shown in Table 2

Fig. 8 Time-history curves of model board uplift

Table. 2 Final uplifting amount of model board (cm)

Measure points	Δh_{EN}	Δh_{ES}	Δh_{WS}	Δh_{WN}	Δh_C
Sign post (P)	25	27	24	25	26
Support column (Z)	27.0	27.5	24.5	26.5	26.0*

Note: The value of "*Sign Post P*" is the uplifting amount of the model board measured by the post, the value of "*Support column Z*" is the distance between the column foot bottom and the ground after the sand deposit is dug.

According to the time-dependent curves of model board uplifting in Fig. 8, it can be concluded that:

In the period of 0 min to 430 min, no uplifting for model board, there was a little deviation in the curves of tube segment uplifting due to a slight increase of water level. After the time point of 430 min, the tube segment began to uplift according to the test results of 5 measured points. It was proven that the tube segment uplifting start time was 430 min, and uplifting was continued until the end of the test.

After the test, through the observation of sand deposit dug out (as shown in Fig. 9), it could be seen that the tube segment was located on the sand deposit completely. The final uplifting amount of posts and the supporting columns were measured and the test results are shown in Table. 2. It was found that the post uplifting amount was close to the supporting columns uplifting amount, which showed the measurement of posts was accurate and effective.

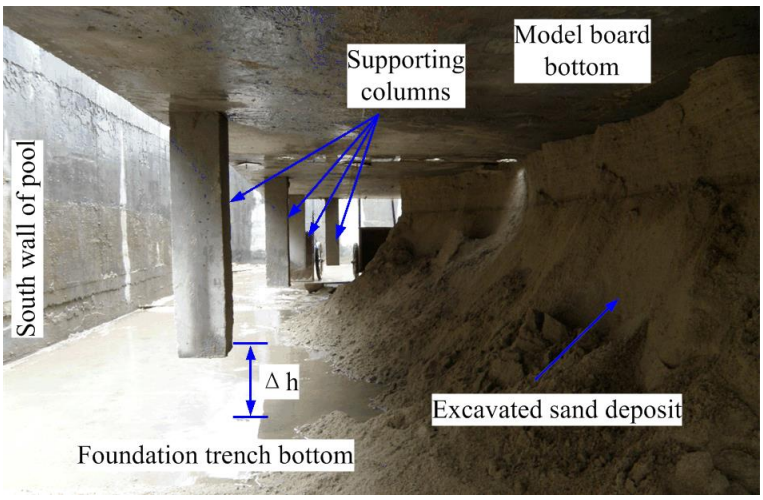

Note: The final uplifting amount *⊿h* is the distance between the supporting columns and the foundation bottom after the test.

Fig. 9 Support column with uplifting after T-UP test

The 5 uplifted time-history curves were almost overlapped. The difference of the uplifting amount was 0 cm to 6 cm at the same time in different positions, the maximum pitch and heeling rate were 0.77% and 0.63% respectively, the maximum relative error between the final and the average uplifting value of the tube segment was 6.3%. The measurement value 26.0 cm at the center of the tube segment was used as the final uplifting amount.

4.2 Expansion rate of sand deposit

The curves on the X, Y axis extension of sand deposit radius were measured in T-UP and T-ST experiments, and were shown in Fig. 10.

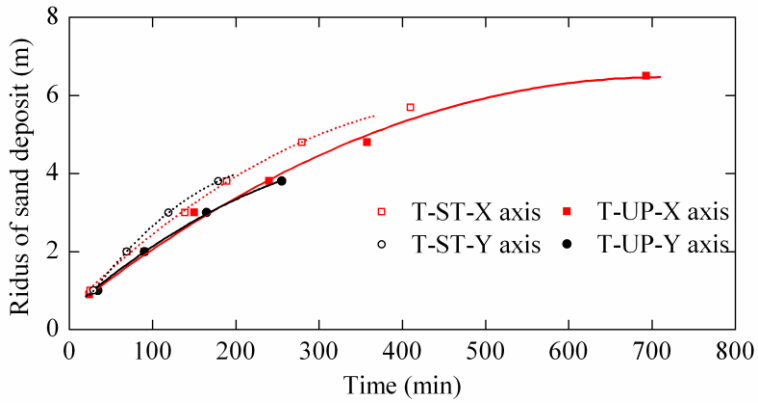

Fig. 10 Time-history curves of sand-deposit radius

The data of T-UP curve conform to the law of quadratic curve, the formula as follows,

$$r = At^2 + Bt + C \quad (1)$$

where, r is sand deposit radius ; t is experiment time ; A, B, C are fitting parameters (as shown in Table. 3).

Table. 3 Fitting parameters of sand-deposit expanding radius

Sand deposit axis	Fitting parameters			
	$A/\times10^{-5}$	B	C	R^2
X	−1.058	0.0157	0.651 4	0.993 00
Y	−2.967	0.0212	0.318 8	0.999 79

Note: R is the correlation of fitting cure.

According to Table. 3, the correlation of fitting cure was excellent for the goodness of fitting, and R^2 was all above 0.99. Time and the extension radius of sand deposit were in conformity with the relationship of convex conic. The growth rate of sand deposit expansion decreased as the increasing of sand deposit radius, which obeyed to the general law in sand deposit extending process (Fang 2012).

By comparing the curves of two experiments in Fig. 10, the X and Y curves in each group (R < 3.8 m) were almost overlapped, the sand deposit expanded to the same radius at the same time in different directions. After test, the final radius of sand deposit in direction of W and E were 650 cm and 700 cm respectively, and the difference of extended radius was small at about 50 cm.

4.3 System water pressure

The time-history curves of water pressure around pump outlet in the T-UP and T-ST experiments were shown in Fig. 11.

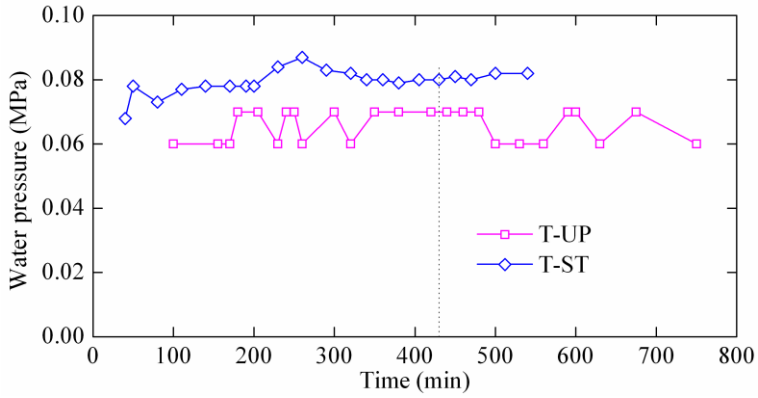

Fig.11 Time-history curves of water pressure of sand pump

According to Fig. 11, the water pressure around pump outlet increased rapidly at the beginning of test, and then maintained at a stable level. The average water pressures of the T-UP and T-ST tests were 0.066 MPa and 0.079 MPa respectively, the maximum relative water pressure increment for both tests appeared at 17% and 20% respectively. Above all, there was no significant change of water pressure in the process of test including the critical moment (430min) and the process of model board uplifting.

4.4 Trench gap water pressure

During construction, the sand deposit was expanding in trench gap, the fluid boundary condition of the gap, flow field in clearance changed, and water pressure of trench gap also changed accordingly. Using the water pressure gauge in trench gap, the influence of test time on water pressure in tests of T - UP, and T - ST could be obtained as Fig. 12.

(a)

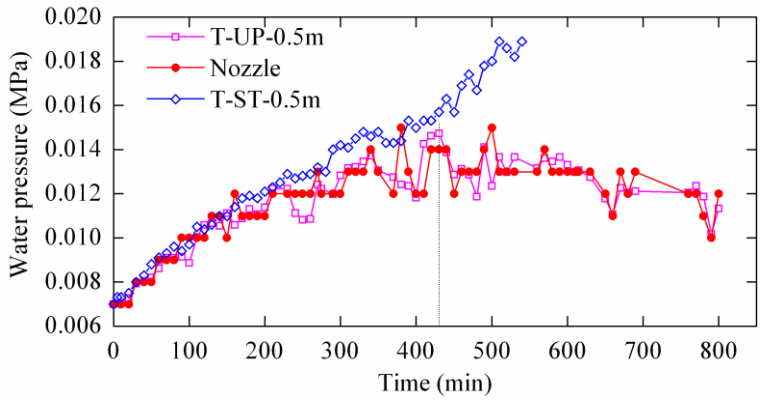

(b)

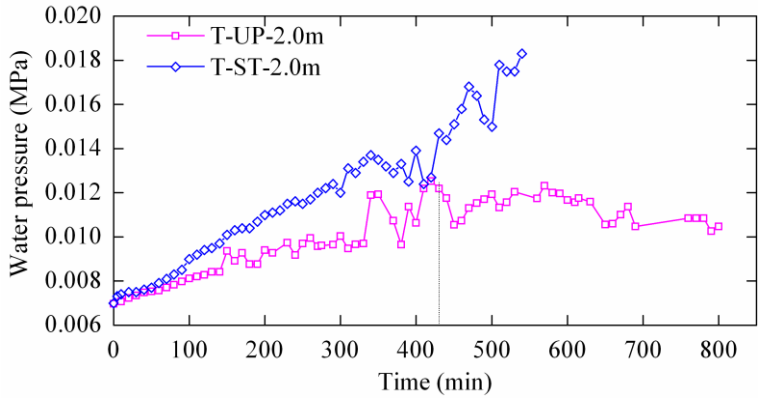

(c)

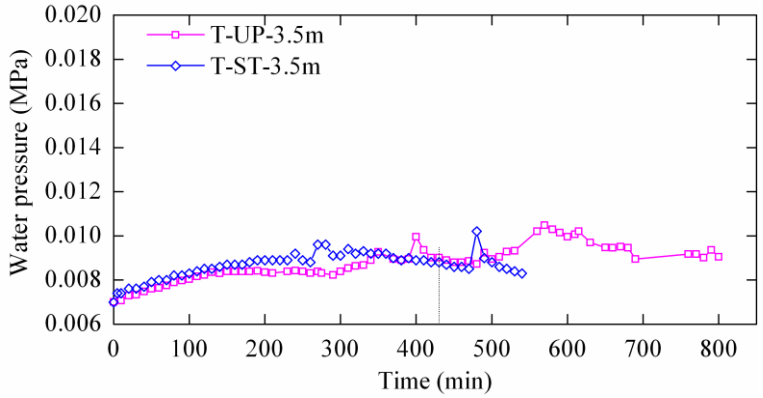

(d)

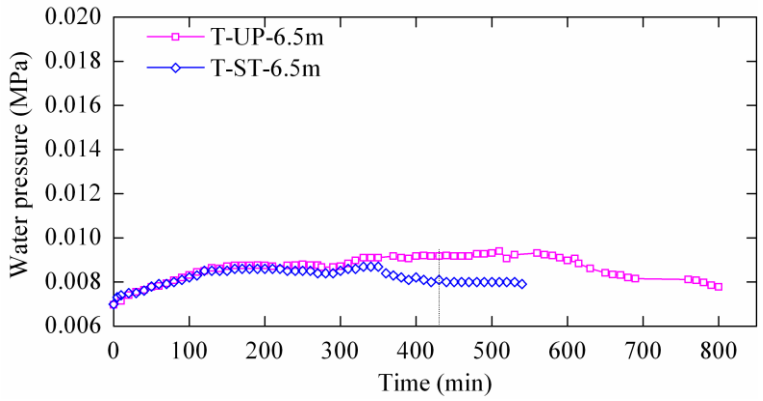

Fig. 12 Time-history curves of water pressure under model board. **(a)** Radius of 0.5m, **(b)** Radius of 2.0 m, **(c)** Radius of 3.5m, and **(d)** Radius of 6.5 m.

In the primary test, the water level of test rose to the overflow hole gradually because of pumping of sand-flow, which resulted in a small growth in water pressure of trench gap during the period of 0 minute to 120 minutes.If the influence of the ascent of tank water level was ignored in the initial test, the water pressure at trench gap increased with the increase of test time from sand outlet along the radial to the model deposit peripheral. For example, in T-UP test, water pressures at 0.5, 2.0, 3.5 and 6.5m radius of sand deposit started to rise at 15, 120, 300 and 500 minutes respectively. In T-ST test, it was also found the same rule.The increase in water pressure values at the trench gap increased volatility. The fluctuation degree of water pressure generally

decreased with increasing sand deposit radius (as shown in Fig. 12). Greater volatility and faster frequency fluctuation of water pressure were observed in the semi-late test period than in previous tests at corresponding position. The fluctuation of water pressure was more intense in T-UP test than in T-ST test.

In T-UP test, the water pressure at trench gap reached its peak in the middle of the test, fluctuated near the peak, and then somewhat decreased in the late test. However, the water pressures in T-ST test showed a single upward trend. The water pressure peak under the model board bottom was found to be related to the model board uplifting process.

5. RESULTS ANALYSIS

5.1 Model board uplifting mechanism

According to the model board uplifting process, the model board was uplifted at the middle stage of the sand-flow method and continued to rise until the end of the test. The uplifting process of the model board can be divided into three sub-stages: I (pulsatile-up stage), II (rapid-up stage), and III (smooth-up stage) based on the characteristics of the uplifting time-history curves (as shown in Fig. 8). The uplifting indicators of each stage are summarized in Table. 4. Each stage has different model board mechanical characteristics, sand particle sedimentation models, and sand deposit structure characteristics, as shown in the following.

Table. 4 Uplifting index of model board

Uplift stage	Time (min)	Gap height (cm)	Uplift mount (mm)	Uplift ratio (%)	Uplift velocity (mm/min)
Start	430	100			
I			20	7.7	0.17
end	550	102			
II			160	61.5	1.52
Start	655	118			
III			80	30.8	0.57
end	795	126			

5.1.1 Uplifting stage I

During this stage, the sand-water mixture under the model board bottom was the medium of the vertical force, which transferred the model board weight from the column feet to the sand deposit. The water pressure fluctuation on the model board bottom aggravated gradually. The model board weight was supported by the sand deposit surface gradually for the translation of the model board supporting system. This condition caused the lower formed sand deposit to be compacted gradually.

Meanwhile, the range of the gap and the thickness of chute and gap respectively became narrower and thinner upon loading on the model board. The transmission process of the sand-flow was smooth. Most sand particles were pumped into the crater and leaked to the sand deposit periphery through the chutes to form an oblique layer accumulation. However, the velocity of the sand-flow increased because the chute

thickness decreased. This thinning, in turn, caused the sand particles to be transported farther and the growth rate of the sand deposit radius to slow down. As the model board was pulsing, the sand and water mixture increased, whereas the thickness of chute decreased. Small sand particles were deposited on the bottom of the model board (the top of the sand deposit), which caused the beating and slow uplifting of the model board. The model board uplifting amount (20 mm) accounted for only 7.7% of the total uplift amount at this stage, and the average uplifting rate was approximately 0.17 mm/min (as shown in Table. 4). The model board pulsed up slowly at this stage.

5.1.2 Uplifting stage II

When the support column feet were completely off the ground, the weight of the model board was supported by the sand deposit, and the test entered uplifting stage II (rapid-up stage). During this stage, the main distribution regularities of the gaps and chutes could be obtained as follows: both were distributed on the top surface of the sand deposit; the flow gaps were the continuation of the crater top surface; and the chutes were the flow gaps continuation distributed around the gaps irregularly, consistent with the basic rules given in other studies (Fang 2012, Mo 2012).

The following results on gaps and chutes were obtained in uplifting stage I through excavation and observation.

The gaps area that connected the crater and chutes was small and was only distributed in a circular area with approximately 1.2 m radius. The thickness of the gap was 1.0 cm to 5.0 cm near the top of the sand deposit.The widths of the chutes were unequal and ranged from 1.2 cm to 15.0 cm. The thickness of chutes was thin in the range of 0.2 cm to 1.0 cm, and a large quantity of chutes was non-uniformly distributed on top of the sand deposit. The sand-flow followed the flow of conservation, although the total cross-sectional area of the flow channel was reduced in the uplifting process (Victor 1998). Hence, the chutes were scoured by the sand-flow more violently, and the chutes were redistributed from sparse to intensive gradually in the dynamic deposition and scour processes.

The sand-flow transportation process was not smooth at this stage, which was beneficial for the deposited sand particles. Most sand particles were conveyed by flow gaps and chutes and deposited on both sides of the thin and wide chutes. These particles then formed an evident horizontal thin layer structure with 0.5 cm to 1.5 cm layer thickness. This condition resulted in a large model board uplifting amount (160 mm) that accounted for 61.5% of the total uplifting amount. The average uplifting speed was 1.52 mm/min at this stage. The number of chutes increased gradually, and the sand-flow velocity decreased in contrast to that in stage I for the scouring action. Some sand particles were transported from the chutes and deposited near the range of the sand deposit, which increased the growth rate of the sand deposit radius.

The shape and trace of the crater, gaps, and chutes, as well as the structural characteristics of sand deposits with level and oblique layered textures, were determined under the model board (as shown in Fig. 13).

(a)

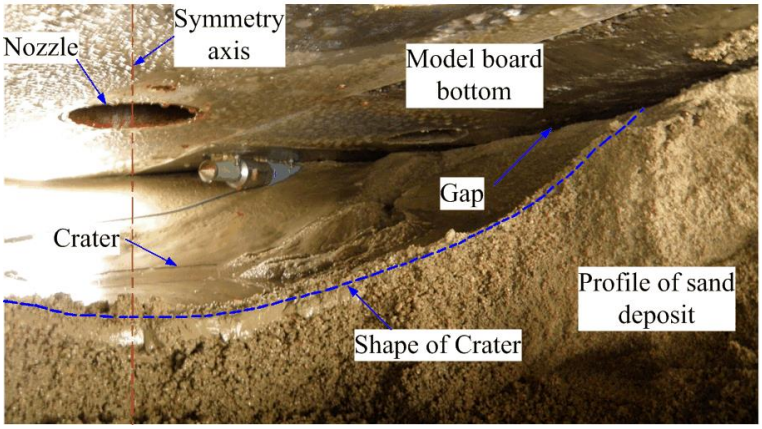

(b)

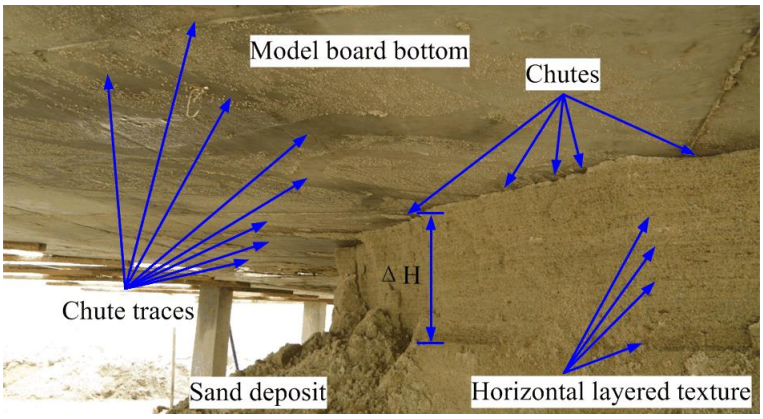

(c)

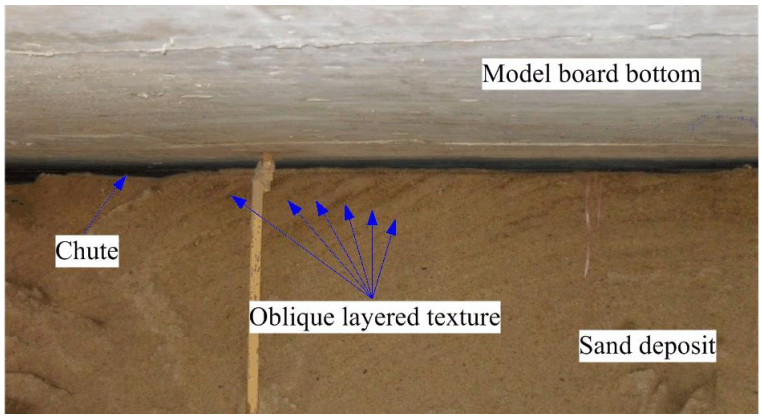

Fig. 13 Excavation situation of sand deposit. **(a)** Crater and gap in T-ST test, **(b)** Chute and horizontal layered texture in T-UP test, and **(c)** Chute and oblique layered texture in T-ST test.

The consistency of the sand deposit was basically defined because the compaction process occurred during uplifting stage I. No further change in the sand deposit consistency was observed at this stage because the model board weight was supported by the sand deposit. The consistency of the horizontal sand layer was denser because each thin sand layer was formed under the vertical stress of the model board at this stage. The uplifting rate increased significantly, the uplifting amount

increased rapidly, and the pulse amplitude became smaller, which were the main signs of uplifting stage II. Most thin layer level structures on the sand deposit top surface formed at this stage.

5.1.3 Uplifting stage III

After the chutes had redistributed in the plane, the test entered stage III of uplifting (smooth-up stage). The sand deposit top surface was covered by meandering, dense, thin, and wide chutes for chute redistribution. The area of the chutes accounted for more than 30% of the deposit top surface area after excavation.

Parts of the sand particles in the sand-flow were deposited on the top surface near the chutes, and the other sand particles were transported to the outer surface of the sand deposit. Sand particles were uniformly distributed at the bottom of the board model for the chutes characterized by low thickness, width, and dense distribution, which uplifted the model board horizontally (the maximum rate of heeling was 0.77%). A considerable amount of sand particles was delivered to the sand deposit periphery at this stage, which produced a comparatively small model board uplifting amount (80 mm) that only accounted for 30.8% of the total uplifting amount. Meanwhile, the uplifting rate decreased to 0.57 mm/min.

During this stage, sand particles were deposited in the level layer and accumulated in the oblique layer simultaneously. The plane distribution density of the chutes was not further changed, but the distributed position was changed. The uplifting rate of the model board was slow, and the beat frequency of the uplifting was small.

The exponential function fitting equation of uplifting process phases II and III are as follows,

$$h=-1647.4\exp^{(-t/134.6)}+129.9 \qquad (1)$$

$$R^2=0.95193$$

where h is the height of sand deposit (cm), t is the test time (min).

However, the consistency in the upper layer was evidently denser than that in the middle and lower layers. Fig. 9 and Fig. 13(b) show that the self-stable angle in the lower layer of the sand board was approximately 36°. An approximately 25 cm to 35 cm thickness of the sand layer on the upper layer of the sand deposit with good orthostatic was called the hard shell layer. From the overlying crust thickness, which was similar to the elevation of the model board, and the clearly horizontally layered texture, the hard shell layer was determined to be the additional dense layer superimposed on the sand deposit top surface under the condition of the model board loading in the uplifting process.

5.2 Sand deposit propagation rules

In Fig. 10, the demarcation time point of the model board uplifting was 430 min. The average growth rate of the sand deposit radius before model board uplifting was 2.3 times that of the rate after the board was uplifted by Eq. (3),

$$\overline{V}=\Delta y/\Delta \qquad (2)$$

where $\overline{V}$ is the average growth rate of the sand deposit radius, Δy is the radius increment of sand deposit pre and post uplifting (m), and Δt is the time increment pre and post uplifting (min).

Comparing the expansion curves of the sand deposit radius in the T-UP and T-ST tests, the expansion curves of the T-UP test gradually deviated from the conventional extension curves (the T-ST) with increasing sand deposit radius. For instance, when the sand deposit radius reached 3.0, 3.8, 4.8 and 5.7 m, the time consumption difference between the two tests increased gradually. The corresponding values were 29, 64, 61 and 77 min. Based on the height extension X5 to X8, the curves of the sand deposit were discontinuous in Fig. 14. The 4.8 m to 7.5 m radius sand deposit extension was also blocked, such that the trench gap could not be fully filled.

(a)

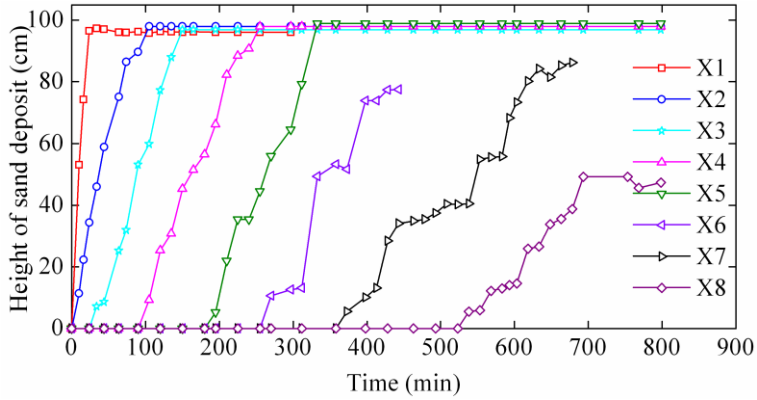

(b)

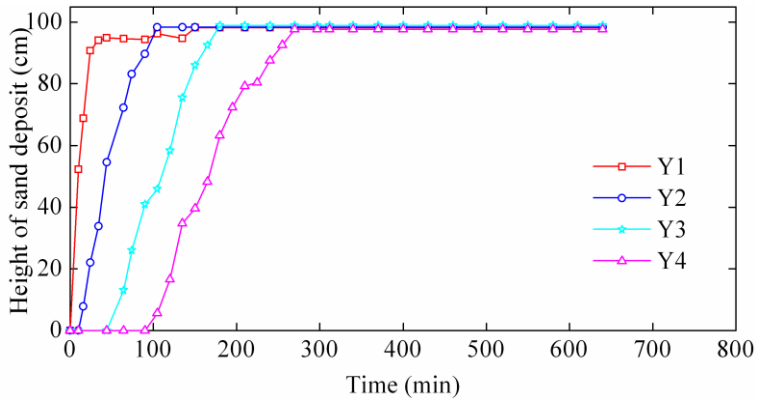

Fig. 14 Time-history curves of sand deposit height. **(a)** X axis, and **(b)** Y axis

All these conditions indicate that the extension of the sand deposit radius was influenced significantly by the model board uplifting process. Less sand particles were transported to the sand deposit periphery because the model board underwent sedimentary compaction, which affected the sand particles in uplifting stages I, II, and III. This condition caused the sand deposit height to increase and the extension rate of sand deposit radius to slow down or even stagnate. The expansion rate of the sand deposit in the radius direction was indirectly influenced by the thin width and intensively distributed chutes because the chutes changed the deposit direction of the sand particles and promoted sand particles deposition.

The sand deposit expanded at the same rate in all directions before model board uplifting. For instance, the time difference value of the X- and Y-axis extensions when the sand deposit extended to 3.8 m radius in the two group tests were 15 and 10 min, respectively (as shown in Fig. 10). The sand deposit height extension curves Y1 to Y4

and X1 to X4 in Fig. 14 indicate that the trench gap can be filled continuously and smoothly. All these observations show that the expansion rate of the sand deposit in this direction was similar before model board uplifting. No significant influence on sand expansion was observed in terms of uniformity and radius.

A large amount of sand particles was uniformly deposited at the model board bottom because clouded chutes were redistributed on the plane when the model board was uplifted. This scenario caused the model board to be vertically uplifted. Other sand particles were evenly transported to the sand deposit periphery and formed a sand deposit with a uniform horizontal radius. These conditions indicate no significant influence on the equilibrium of sand deposit extension in the uplifting process.

The uplifting process of the model board lasted for approximately 365 min, the increment of the sand deposit radius was 110 cm, the average extension rate of the radius was 0.30 cm/min, and the ratio of the sand deposit radius increment and model board uplifting amount was approximately 5:1. Finally, the sand deposit radius was 650 cm to 700 cm, which was slightly less than the design value of 750 cm. The corresponding uplifting amount was 26 cm.

The final fullness of the sand deposit top surface in the T-UP test was obtained based on Eq. (4) (Mo 2012).

$$f_A = A_{sd} / A_{mb} \times 100\% = (125 - (0 + 7.5)) / 10.12 \quad (3)$$

where f_A is the fullness of sand deposit top surface, A_{sd} is the effective area of sand deposit top surface, A_{mb} is the model board bottom area. The final top surface fullness of the sand deposit in T-ST test was 96 %.

From the above analysis, the process of model board uplifting was extremely unfavorable for sand deposit expansion, and the sand deposit radius was no longer growing effectively in the uplifting process. Therefore, using the foundation treatment on immersed tunnels with the tube segment to start uplifting as the standard to stop construction in engineering practices is questionable. This scenario can cause the sand deposit radius and the top surface fullness to fall short of the design requirements. Effective measures should be taken to ensure that the sand deposit can extend to the design radius before the tube section is uplifted.

5.3 System water pressure

The total system current was 78 A to 85 A, and the sand pump current was 27 A to 30 A. The output power and flow rate were consistent with the input caused by the sand pump in the tests because the system current had not been changed significantly. Fig. 11 and Fig. 12 indicate that the water pressure under the model board bottom increased constantly, and the influence scope of the sand deposit expanded constantly. However, the water pressure of the sand pump changed slightly. All of these conditions indicate that the water pressure near the pump nozzle was determined by the pump performance (power and lift) during the sand-flow construction (Victor 1998). This observation also had no direct relation to the sand deposit and water pressure under model board.

The water pressure near the sand pump nozzle was basically the same during the uplifting phase because the pumped fluid was free and abided by flow conservation. This scenario was true even when the flow field under model board bottom was changed by the better airtight semi-enclosed spaces and minimum thickness gaps and chutes.

Therefore, the model board uplifting process had no apparent influence on the sand pump in terms of outlet flow and pressure, and no corresponding relationship existed between the water pressure expansion and model board uplifting. Of course, the premise of the test process and discussion was that the sand pump was in normal working condition. Thus, the water pressure of the sand pump under a limited state requires further study.

5.4 Trench gap water pressure

A semi-closed space existed between the model board and the extending sand deposit surface, and its impermeability increased with sand deposit extension. Along with sand deposit expansion, the corresponding water pressure (as shown in Fig. 12) began to rise, and the water pressure within the scope of the original sand deposit also continued to increase. The water pressure in the semi-closed space had been fluctuating because of the interaction between the pumped sand-flow and the sand deposit, gaps, and chutes. By contrast, the velocity and pressure of the fluid outside the sand deposit dropped rapidly because the sand-flow was transported to the free area from the chute outlet.

In the model board uplifting stage, the impermeability of the semi-enclosed space was better because the model board was directly pressed onto the surface of the sand deposit. The thin and dense distribution chutes were blocked and thus collapsed more frequently, which increased both the amplitude and frequency of water pressure fluctuation, particularly in the crater. The tests showed that the water pressure in test T-UP fluctuated more remarkably than in the test T-ST.

After model board uplifting, the increment of the sand deposit radius was very small, the flow gaps mainly redistributed on the plane, and the length of the gaps and the flow resistance caused by the gaps and chutes no longer increased. Thus, the water pressure on the board bottom reached a peak and then increased to a level fluctuation stage around the peak.

Stress analysis was conducted on the model board based on the assumption that the water pressure demonstrated a cylindrical cone distribution. The force diagram of the model board (as shown in Fig. 15) and the force equilibrium condition (Eq. (5))were obtained, where G_i denotes gravity, F_- stands for buoyancy, R is the pedestal supporting force, p is water pressure on the board bottom and A is the influence area of water pressure on the model board bottom.

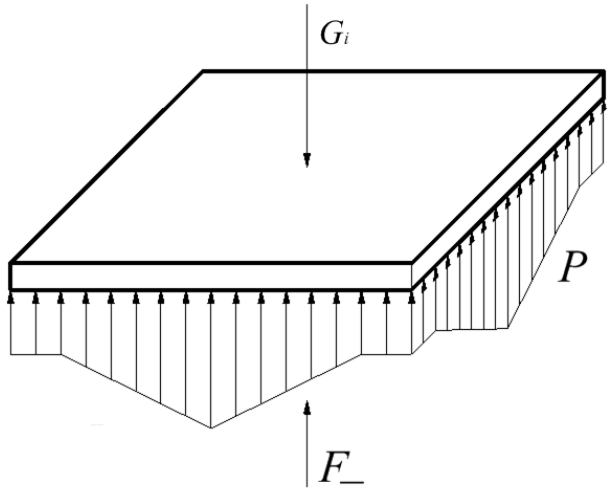

Fig. 15 Force diagram of model board

$$\sum G_i = \sum F_- + \sum R + \iint_A p d\sigma \tag{4}$$

When the water pressure under the model board bottom rose to the corresponding value, the model board was in the stress limit state. The model board could be uplifted because the water pressure under the model board bottom had a small amplitude increment. The test then entered the model uplifting phase.

The experimental results indicate that the final extended range of water pressure on the model board bottom and the moment when the model board began to uplift were determined by the model board weight.

6. CONCLUSIONS

In order to analyse the tube segment uplift on the sand-flow foundation treatment of immersed tunnels, a group of full scale model test was conducted. The conclusions are obtained as follows:

1) The uplifting process can be divided into three sub-stages, each model board has its own mechanical characteristics, sand particle sedimentation model and sand deposit structure. In the process of uplifting, the model board with small instantaneous pulse amplitude is in the state of level uplifting. Through the real-time measurement of the model board uplifting amount and rate in construction, it could be demonstrated that whether the tube section has been uplift or which uplifting stage it is. The uplifting of stage I can be used to reduce the thickness of the gaps and chutes.
2) The uplifting process of model board has no effect on the balance of sand deposit radius expansion, but significantly influences the radius expanding rate of sand deposit. When the model board starts to uplift, there is almost no effective growth in sand deposit radius.
3) The uplifting of model board and the change of water pressure at the bottom of model board show no apparent effect on water flow and pressure at sand pump

nozzle. The water pressure at sand pump nozzle couldn't be used to indicate the uplifting process of tube segment accurately.

4) The water pressure of the trench gap increase volatility with the increase of the sand deposit from the sand outlet to the peripheral of model board along the radial direction. The peak of water pressure at the bottom and the time point of model board uplifting as indicators for construction control are determined by the weight of model board.

ACKNOWLEDGEMENTS

This study is financially supported by National Key Research and Development Program of China (2017YFC1500400), project of National Natural Science Foundation of China (NO. 51438004, 51508119 & 51508200).

REFERENCES

Fang, Y.G., Li, W., Mo, H.H., Gu, R.G. and Chen, J.S. (2012), "Experiment and analysis of law of sand deposit expansion in foundation of immersed tube tunnel treated by sand-flow method", *Chin. J. Rock Mech. Eng.,* **31**(1), 206-216. (in Chinese)

Glerum, A. (1995), "Developments in immersed tunnelling in Holland", *Tunn. Undergr. Sp. Tech*., **10**(4), 455-462.

Guangzhou Municipal Engineering Design & Research Institute (GMED&RI), Maunsell Consultants Asia Limited (MCAL). (2008).

Li, W., Fang, Y.G., Mo, H.H., Gu, R.G. and Chen, J.S. (2013). "Sand deposit-detecting method and its application in model test of sand-flow", J. Cent. South. Univ., 20 (10), 2840-2848.

Li, W., Fang, Y.G., Mo, H.H., Gu, R.G. and Chen, J.S., Wang, Y.Z. and Feng, D. l. (2014), "Model test of immersed tube tunnel foundation treated by sand-flow method", *Tunn. Undergr. Sp. Tech., 40 (2)*, 102-108.

Mo, H.H., Wei L., Fang, Y.G., Chen, J.S.and Gu, R.G. (2012), "Model experimental research on effect of material of immersed tunnel bottom surface on foundation formed by sand-flow method", *Chin. J. Rock Mech. Eng.,* 31(7), 1452-1461. (in Chinese)

Nestor, R., Walter, G. (1997), "Catalogue of immersed tunnels", *Tunn. Undergr. Sp. Tech*., 12(2), 163-316.

Sun, J. (2006), "Discussion on some key technical issues for design and construction of undersea tunnels", *Chin. J. Rock Mech. Eng.,* 25(8), 1513-1521. (in Chinese)

Thomas, R. K. (1986), "Alternative concepts for undersea tunnels", *Tunn. Undergr. Sp. Tech*., **1**(1), 283-287.

Walter, C.G. (1997), "Steel-shell immersed tunnels – forty years of experience", *Tunn. Undergr. Sp. Tech*., **12**(1), 23-31.

Walter, C.G. (2001), "Immersed tunnel settlements – Parts 1: Nature of settlements", *Tunn. Undergr. Sp. Tech*., **16**(3), 195-201.

Walter, C.G. (2001), "Immersed tunnel settlements –Parts 2: Case histories", *Tunn. Undergr. Sp. Tech*., **16**(3), 203-210.